Supporting Information

Enhancing Optical, Dielectric, and Thermal Properties of Bio-based Polyimides Incorporating Isomannide with Bent and Sterically Constrained Conformation

Ririka Sawada and Shinji Ando*

Department of Chemical Science and Engineering, Tokyo Institute of Technology,

Ookayama 2-12-1-E4-5, Meguro-ku, Tokyo 152-8552, Japan

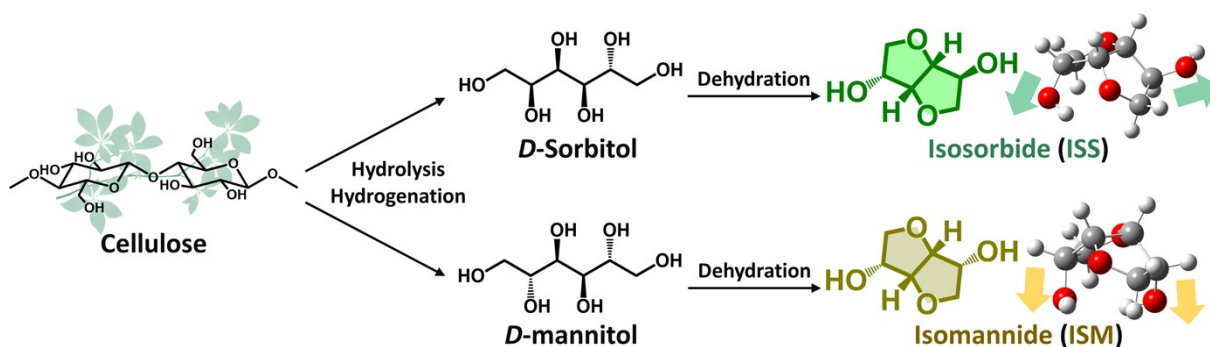*Email: ando.s.aa@m.titech.ac.jp Phone: +81-3-5734-2137

Figure S1. Synthetic scheme and chemical structures of isosorbide (ISS) and isomannide (ISM).
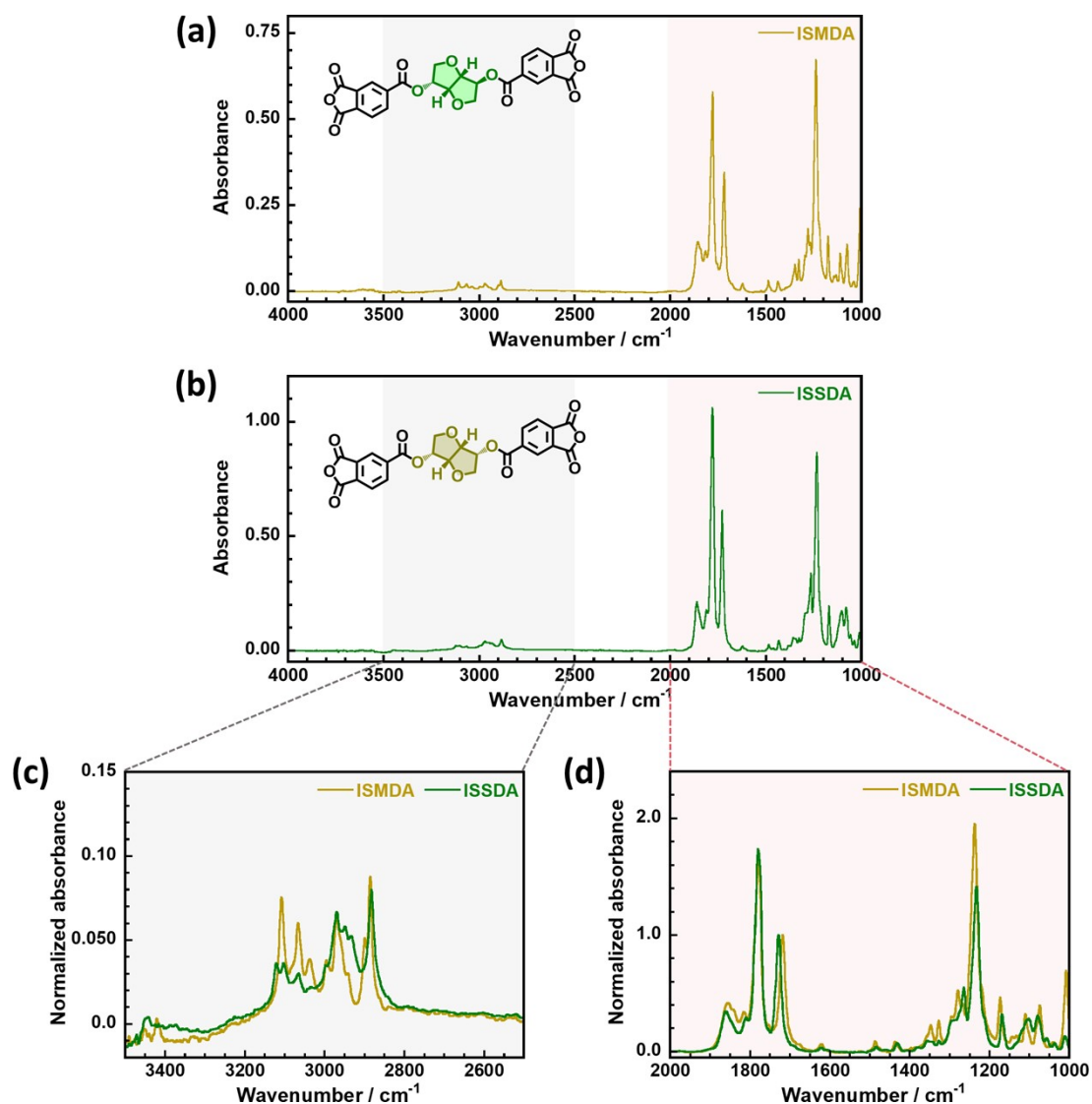
Figure S2. Infrared (IR) spectra of (a) ISMDA and (b) ISSDA by KBr method, and the partial IR spectra at (c) 2500–3500 cm⁻¹ and (d) 1000–2000 cm⁻¹.
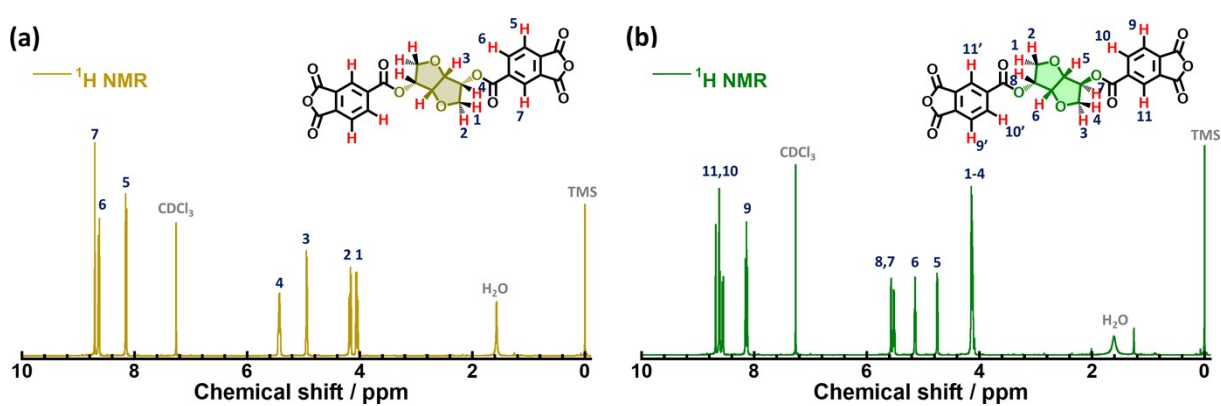

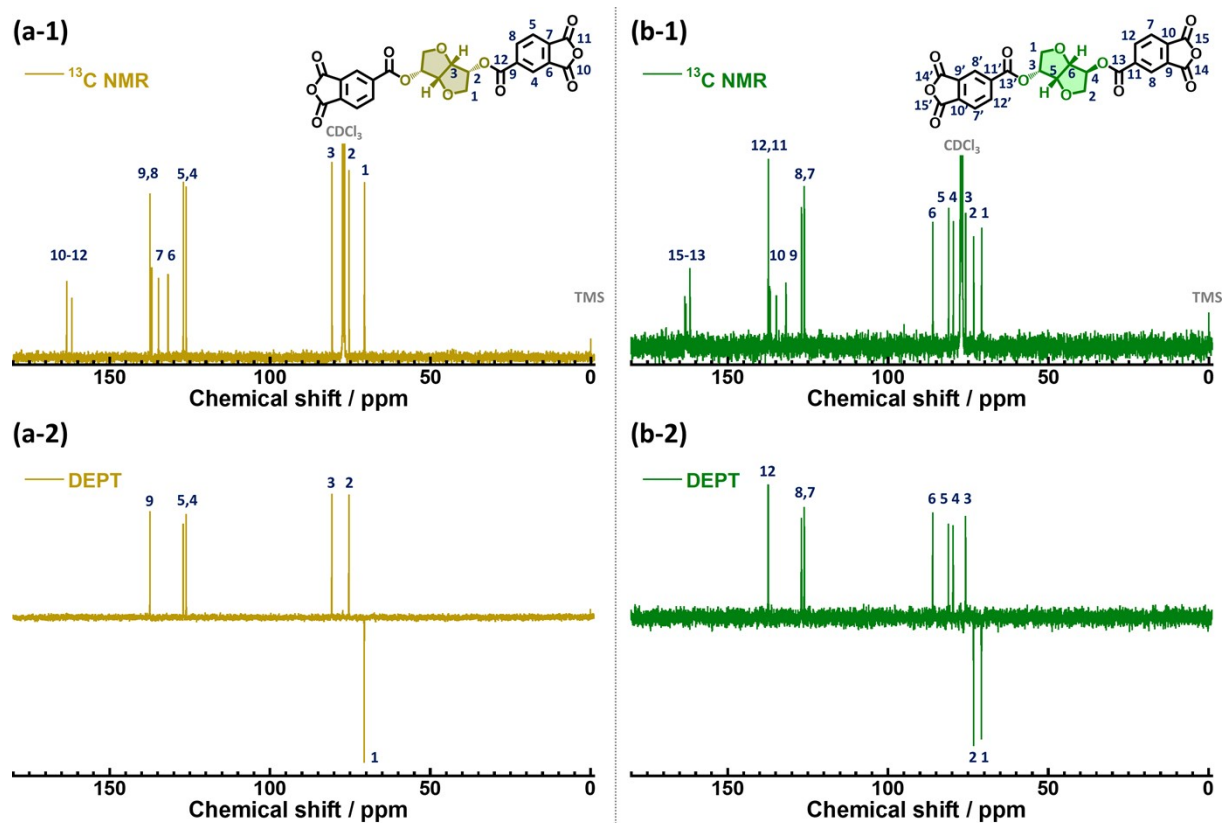**Figure S3.** ¹H NMR spectra of (a) ISMDA and (b) ISSDA dissolved in chloroform−*d*.
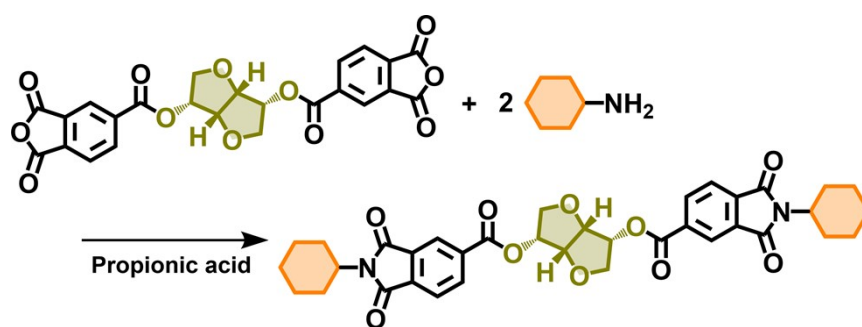
Figure S4. ^{13}C NMR and DEPT spectra of (a) ISMDA and (b) ISSDA dissolved in chloroform−*d*.


**Scheme S1.** Synthetic scheme of ISM-2Ch (model compound, MC).

Table S1. Labels of copolyimides (CoPIs), feed compositions of source materials, and molar contents of ISM (C_m).

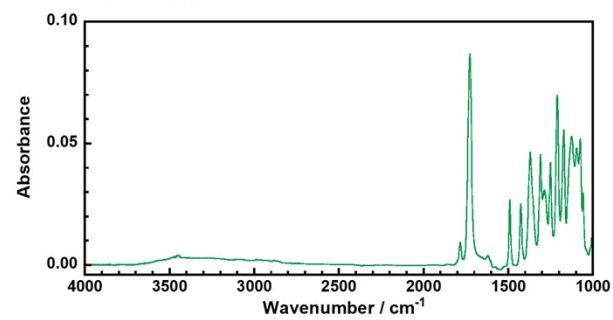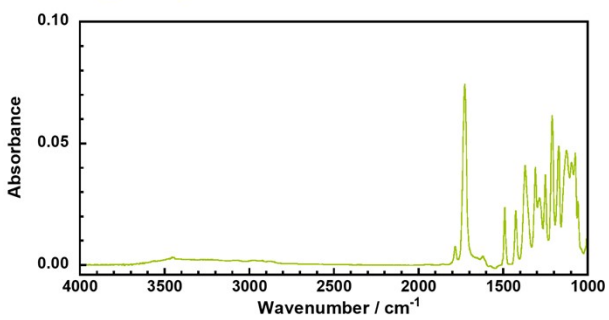| Copolyimide	Molar ratio (ISS:ISM)	ISSDA /mmol	ISMDA /mmol	TFDB /mmol	Molar content of ISM, C_m / %
ISS_9-ISM_1	9:1	0.72	0.08	0.8	10
ISS_8-ISM_2	8:2	0.64	0.16	0.8	20
ISS_7-ISM_3	7:3	0.56	0.24	0.8	30
ISS_6-ISM_4	6:4	0.48	0.32	0.8	40
ISS_5-ISM_5	5:5	0.40	0.40	0.8	50

(a) ISS₉-ISM₁
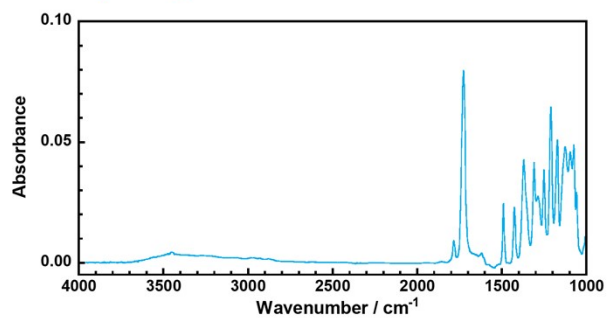
(b) ISS₈-ISM₂
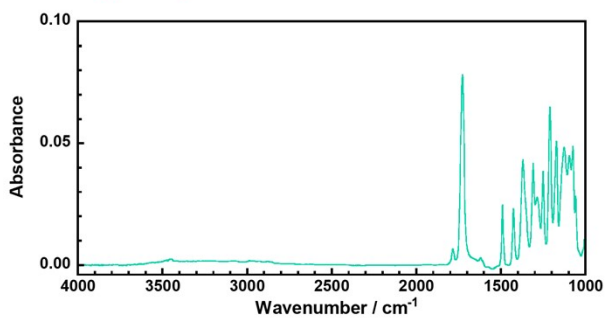
(c) ISS₇-ISM₃

(d) ISS₆-ISM₄
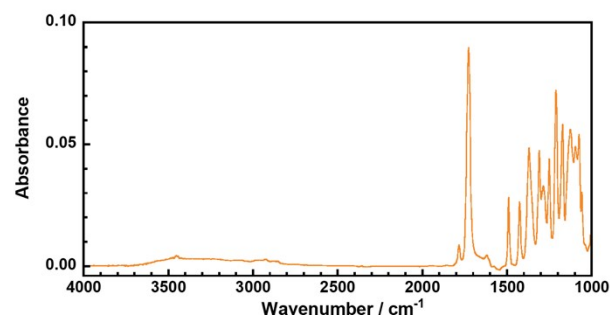
(e) ISS₅-ISM₅

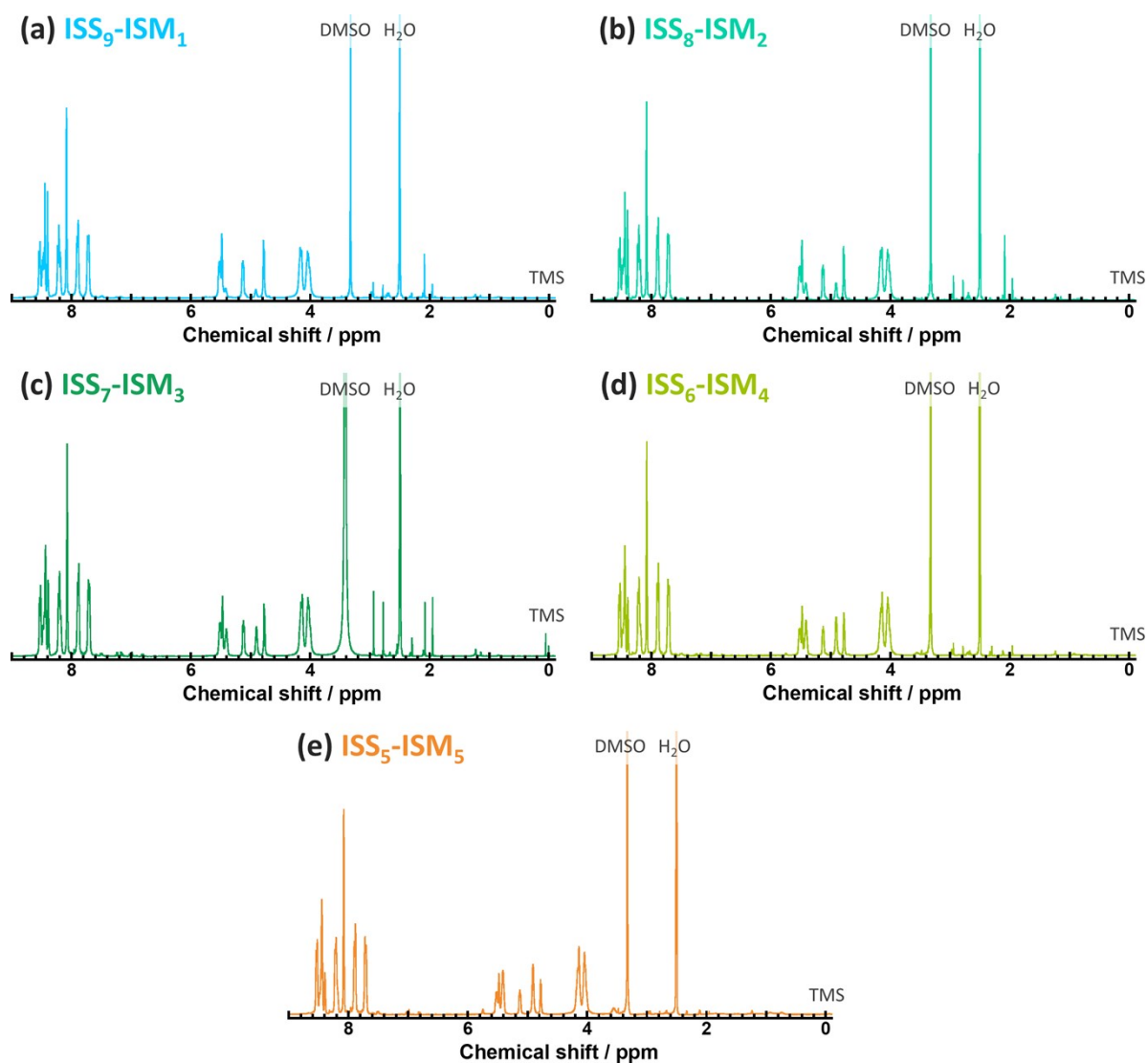**Figure S5.** FT-IR spectra of CoPI films obtained by the ATR method.

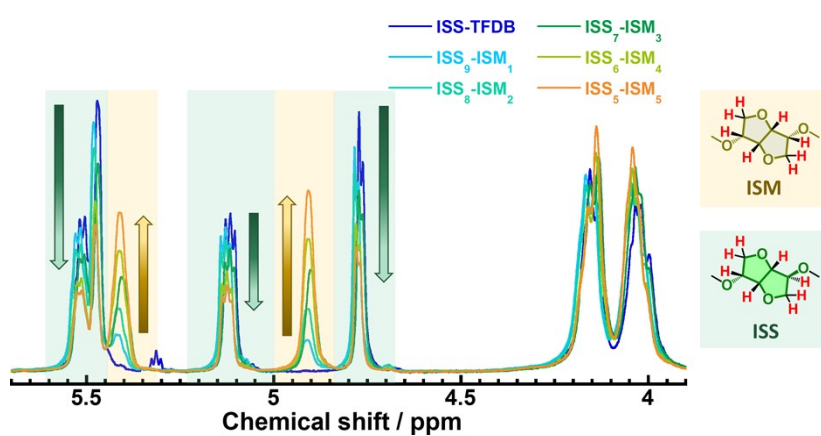**Figure S6.** ^{1}H NMR spectra of CoPIs dissolved in DMSO−d_6.

Figure S7. Spectral changes of ^{1}H NMR spectra of CoPIs dissolved in DMSO−d_6 with an increase in the molar content of ISM.

Table S2. Signal intensities of the characteristic ^{1}H NMR peaks assignable to ISS and ISM of CoPIs in **Figure S7**, and the molar contents of ISM (C_m) estimated from NMR spectra. The signal intensities are normalized with that of the aromatic signal resonated at δ = 8.04 ppm.

Copolyimide	ISS		ISM	Molar content of ISM, C_m by NMR / %
	(a) 4.77 ppm	(c) 5.11 ppm	(b) 4.87 ppm *	
ISS-TFDB	1.01	1.00	–	0.0
ISS$_9$-ISM$_1$	0.90	0.90	0.09	9.0
ISS$_8$-ISM$_2$	0.81	0.81	0.19	19.0
ISS$_7$-ISM$_3$	0.72	0.71	0.29	28.8
ISS$_6$-ISM$_4$	0.58	0.59	0.41	41.2
ISS$_5$-ISM$_5$	0.48	0.49	0.50	50.8

* As the ISM signal contains two types of protons, half of the signal intensities are shown to estimate the ISM content.
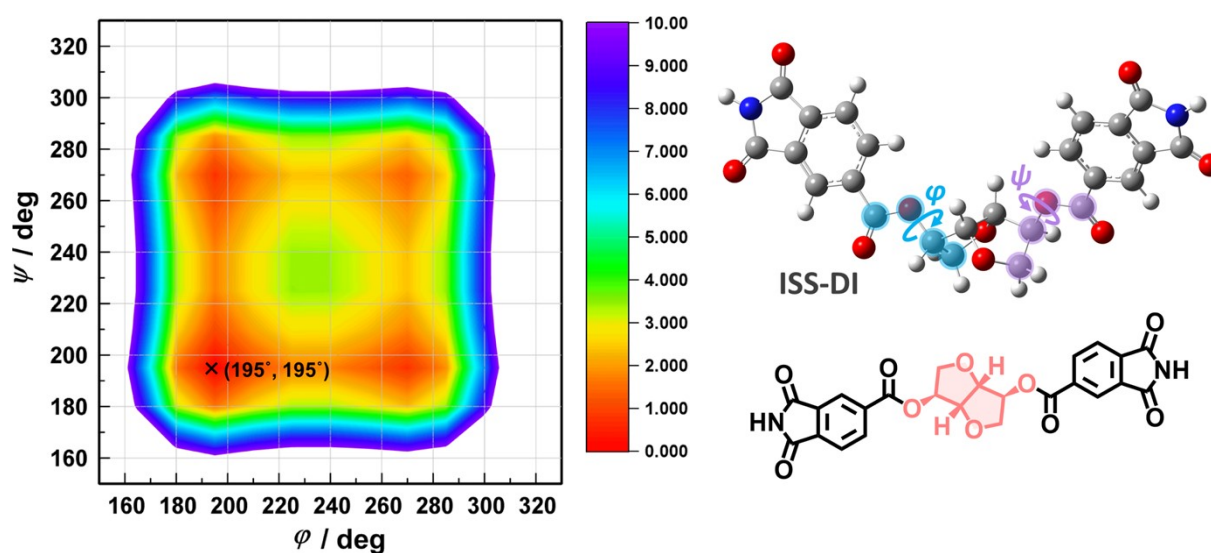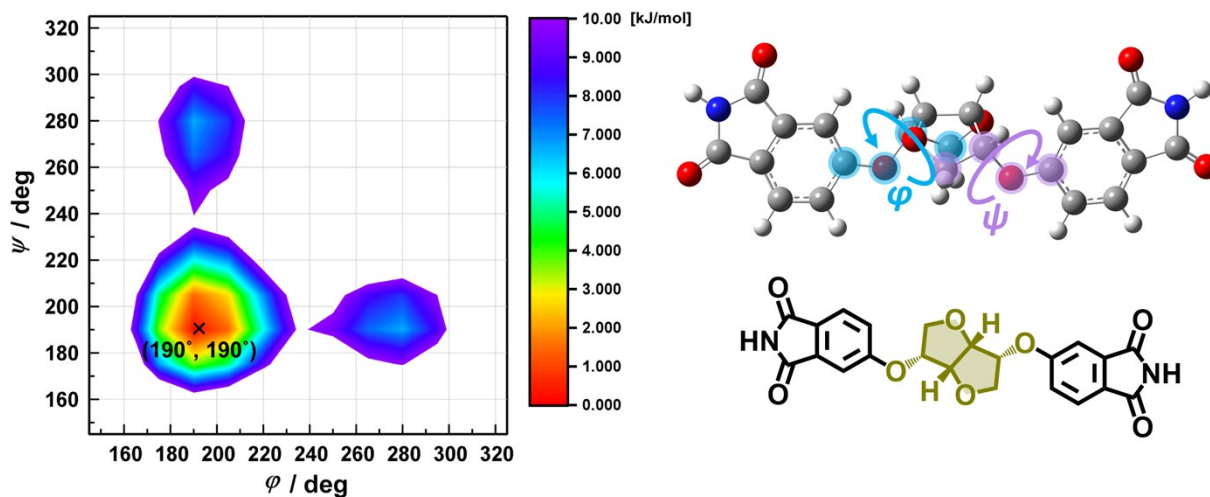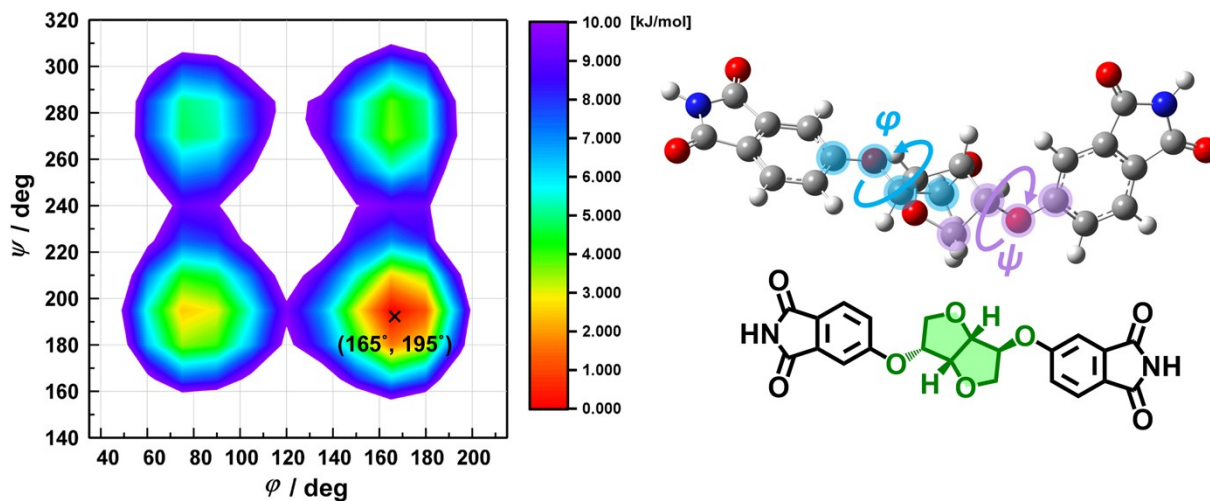

Figure S8. Calculated conformational energy surface and the optimized conformation of ISI-DI.
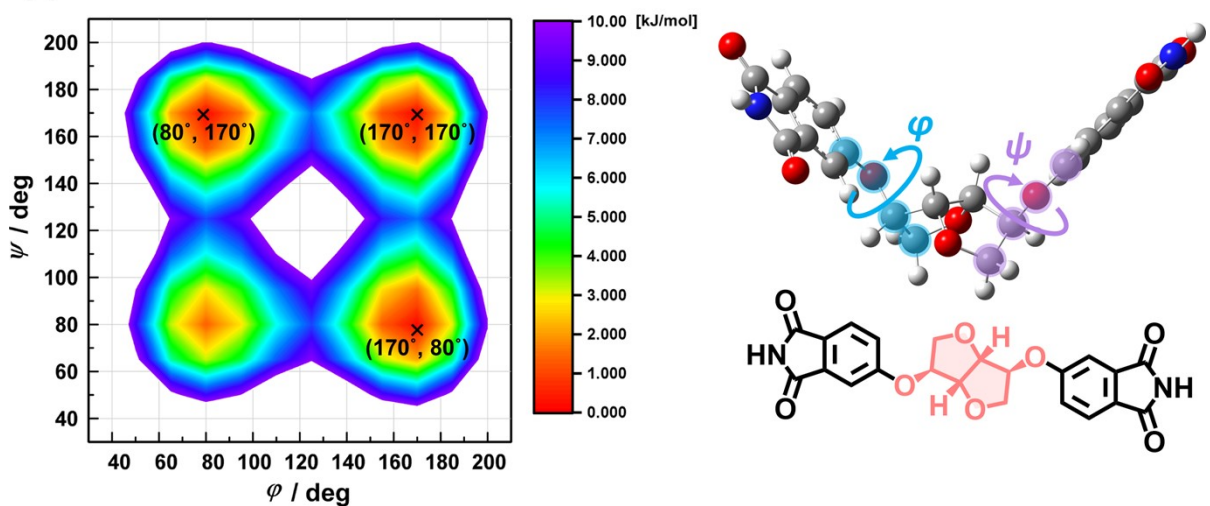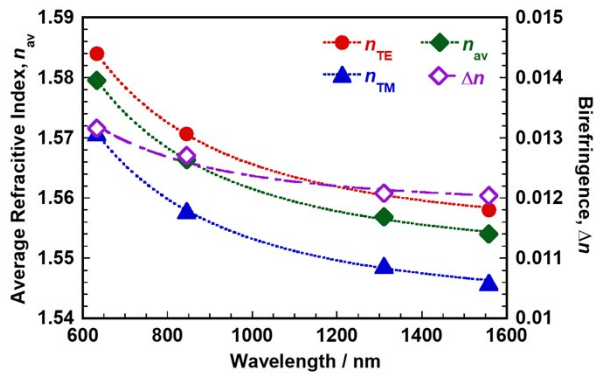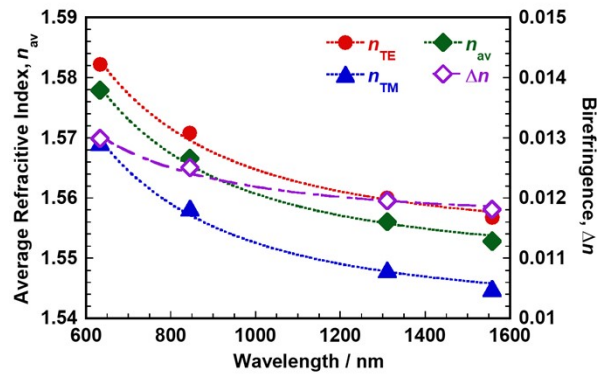
Figure S9. Calculated conformational energy surfaces and the optimized conformations of (a) ISM-et-DI, (b) ISS-et-DI, and (c) ISI-et-DI.

(a) ISS$_9$-ISM$_1$

(b) ISS$_8$-ISM$_2$

(c) ISS$_7$-ISM$_3$
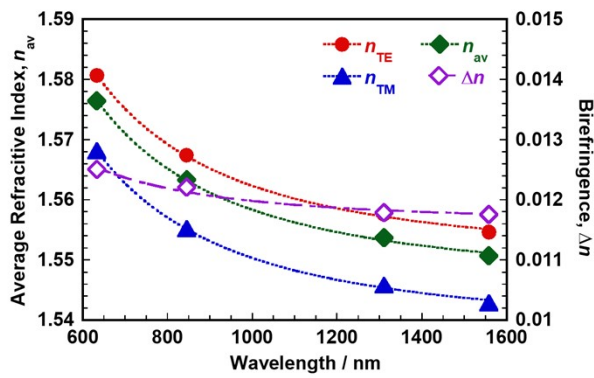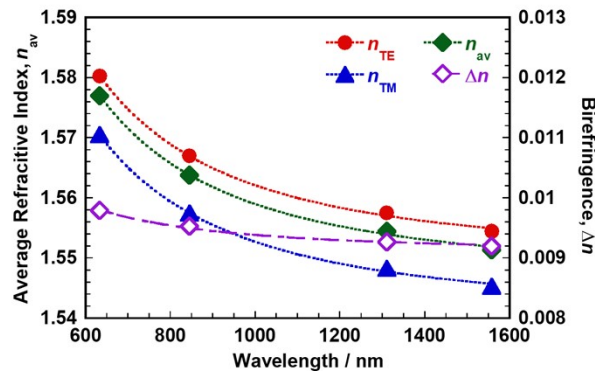
(d) ISS$_6$-ISM$_4$
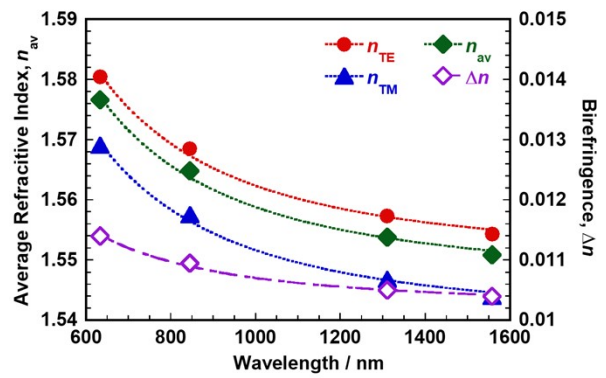
(e) ISS$_5$-ISM$_5$

Figure S10. Experimental wavelength dispersions of refractive indices (n_{TE}, n_{TM}, n_{av}) and in-plane/out-of-plane birefringence (Δn) of ISS-PI films fitted by the simplified Cauchy's dispersion formula.

Table S3. Experimental in-plane, out-of-plane, and average refractive indices (n_{TE}, n_{TM}, and n_{av}, respectively) and birefringence (Δn) of ISS-TFDB (HomoPI) and CoPIs measured at 1310 nm, and the fitted parameters of wavelength dispersion (n_∞, B_n)

Polyimide	n_{TE}	n_{TM}	n_{av}	Δn	n_∞	B_n [a]
ISS-TFDB (HomoPI) [1]	1.5597	1.5467	1.5554	0.0130	1.5475	12875
ISS$_9$-ISM$_1$	1.5609	1.5488	1.5569	0.0121	1.5494	12115
ISS$_8$-ISM$_2$	1.5601	1.5481	1.5561	0.0120	1.5489	11878
ISS$_7$-ISM$_3$	1.5576	1.5459	1.5537	0.0118	1.5462	12168
ISS$_6$-ISM$_4$	1.5573	1.5468	1.5538	0.0105	1.5465	12289
ISS$_5$-ISM$_5$	1.5575	1.5483	1.5545	0.0093	1.5469	12089

[a] Unit: nm^2.
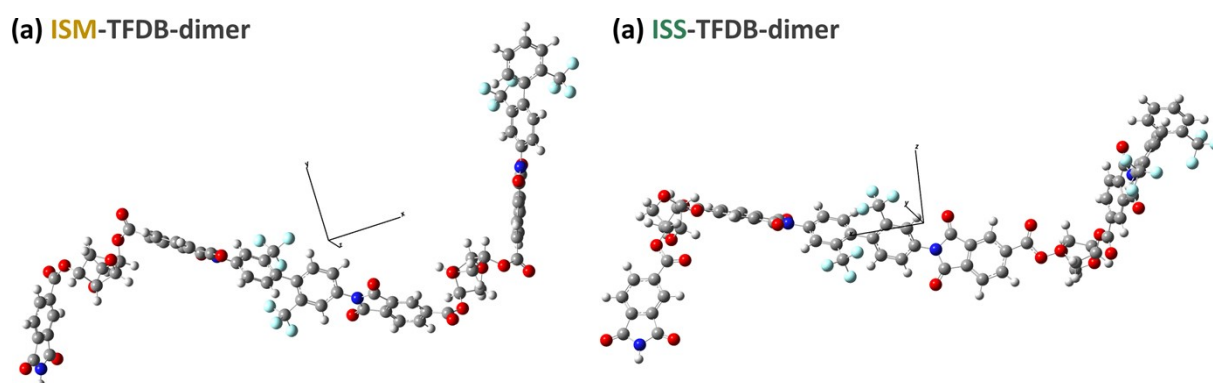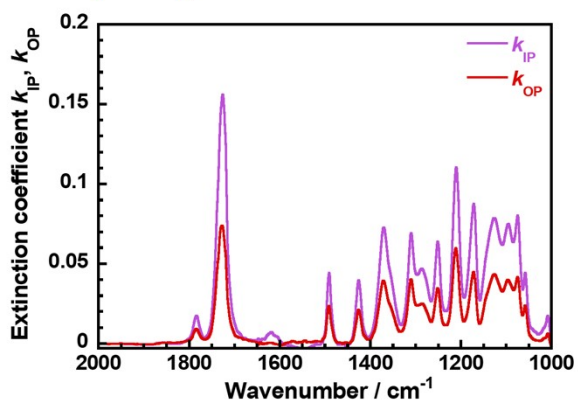
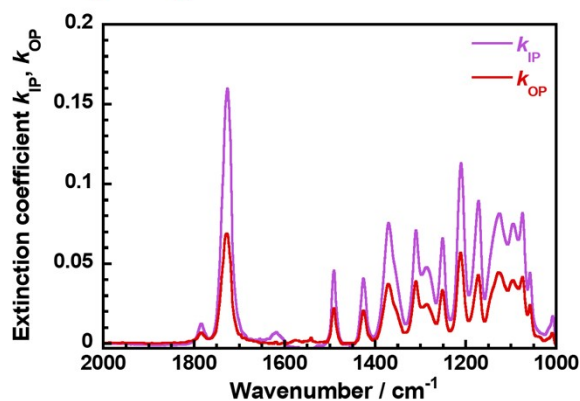**(a) ISM-TFDB-dimer**   **(a) ISS-TFDB-dimer**

Figure S11. Optimized conformations and the principal axes of polarizability tensor of dimer model compounds (MCs) of ISM-TFDB and ISS-TFDB.
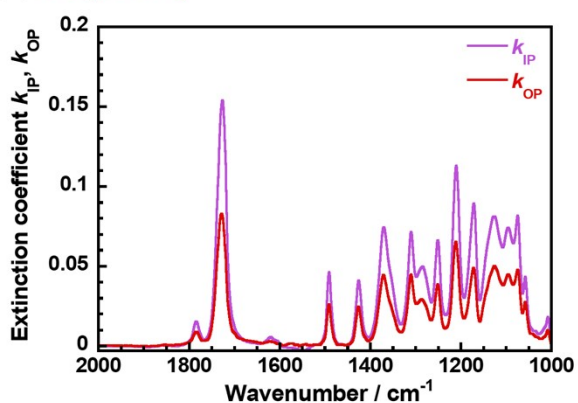
(a) ISS$_9$-ISM$_1$
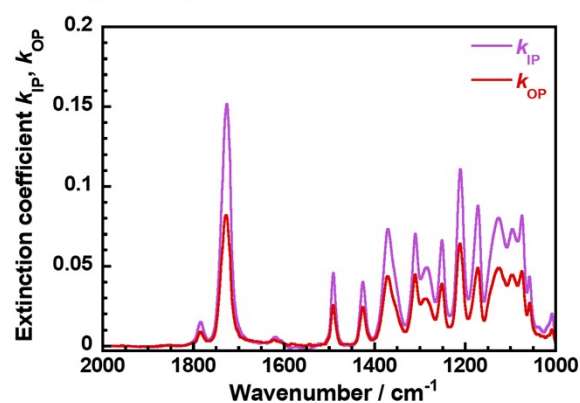
(b) ISS$_8$-ISM$_2$

(c) ISS$_7$-ISM$_3$

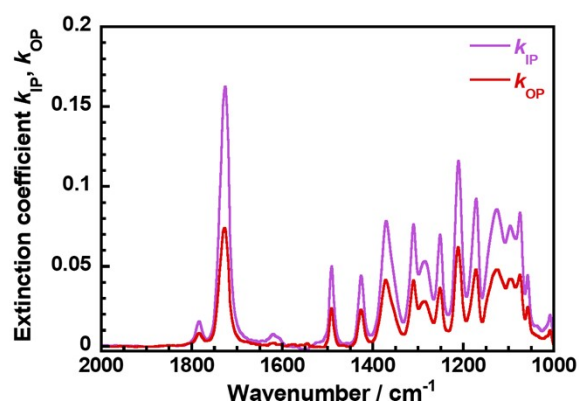**(d) ISS$_6$-ISM$_4$**

(e) ISS$_5$-ISM$_5$

Figure S12. In-plane and out-of-plane extinction coefficient (k_{IP}, k_{OP}) spectra of CoPIs obtained by the polarized ATR-FT-IR method.
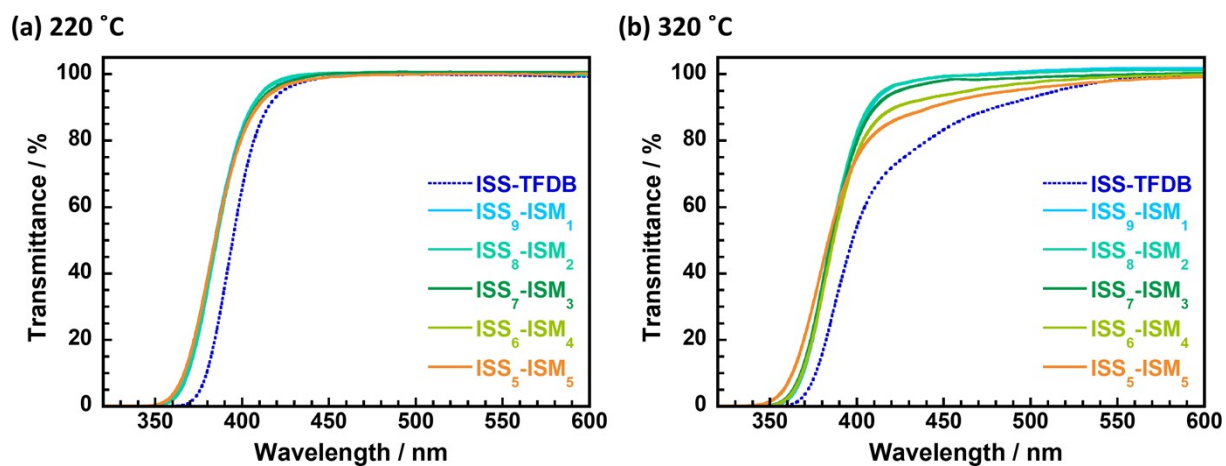
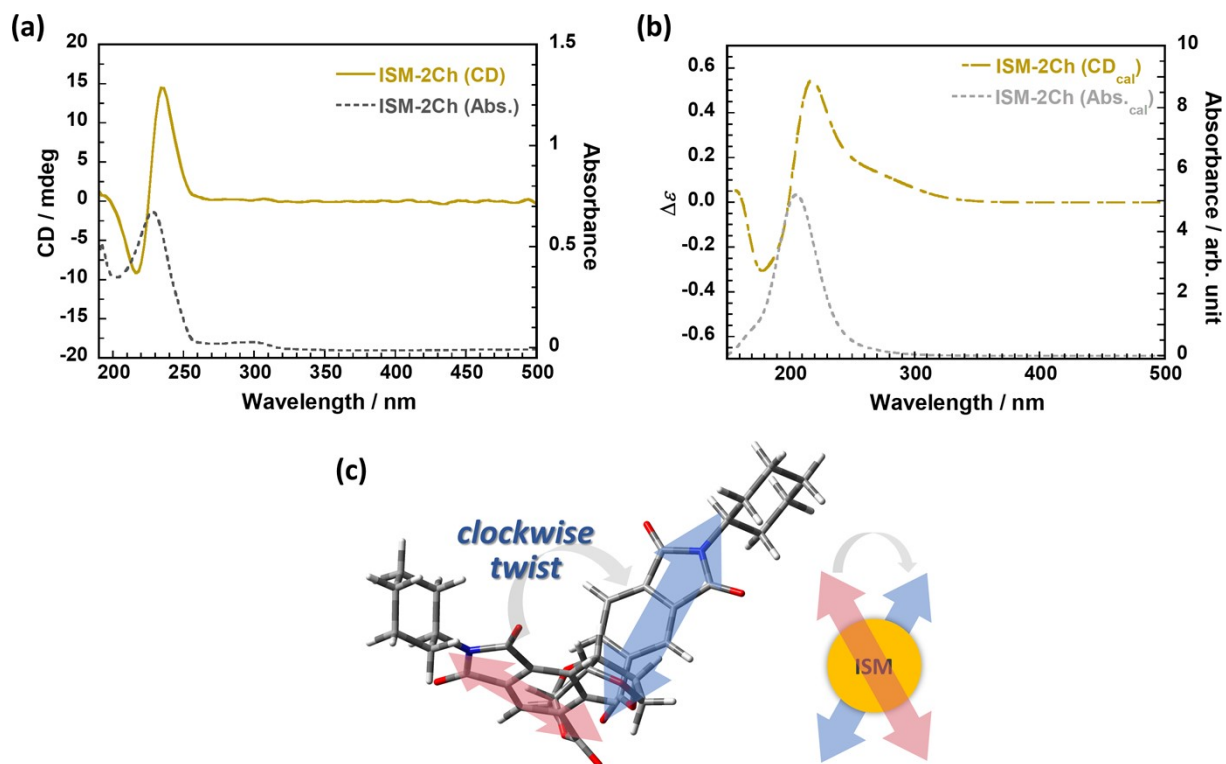**Figure S13.** UV-vis transmission spectra of CoPI films.

Figure S14. (a) Experimental and (b) calculated UV-vis circular dichroism (CD) spectra, and (c) the optimized structure and absolute configuration corresponding to the transition dipoles of a model compound (ISM-2Ch).

Table S4. Film thickness (d), dielectric constants (D_k), dissipation factors (D_f), and contributions of dipolar polarization (P_d) at 10 and 20 GHz.

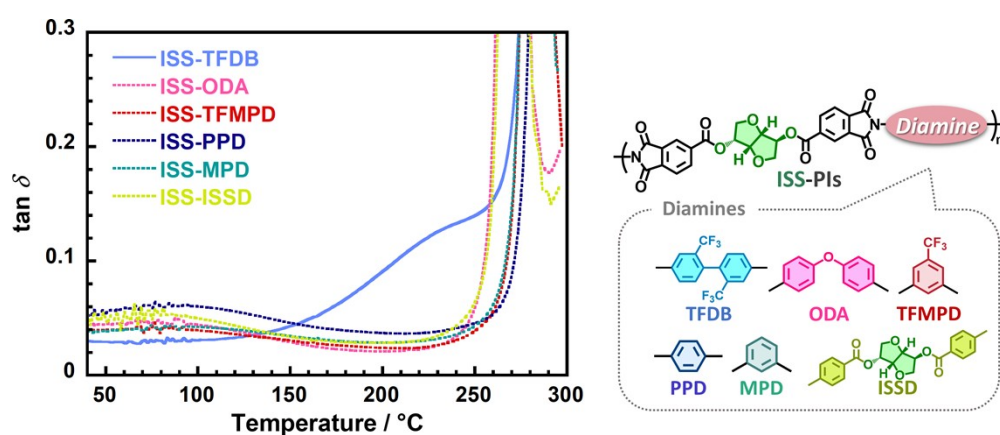| Polyimide	d / μm	D_k		D_f		P_d [a]	
		10 GHz	20 GHz	10 GHz	20 GHz	10 GHz	20 GHz
ISS-TFDB [1]	17.2	2.97	2.94	0.0105	0.0124	0.0752	0.0716
ISS$_9$-ISM$_1$	18.0	2.95	2.90	0.00928	0.0116	0.0721	0.0659
ISS$_8$-ISM$_2$	16.0	2.95	2.89	0.00988	0.0118	0.0725	0.0650
ISS$_7$-ISM$_3$	26.0	2.92	2.86	0.00982	0.0119	0.0699	0.0624
ISS$_6$-ISM$_4$	17.0	3.02	2.96	0.0104	0.0128	0.0820	0.0748
ISS$_5$-ISM$_5$	9.5	2.99	2.97	0.0107	0.0131	0.0769	0.0757

[a] Estimated using Eq. (8).

Figure S15. DMA curves of ISS-PIs derived from ISSDA dianhydride and six kinds of diamines.
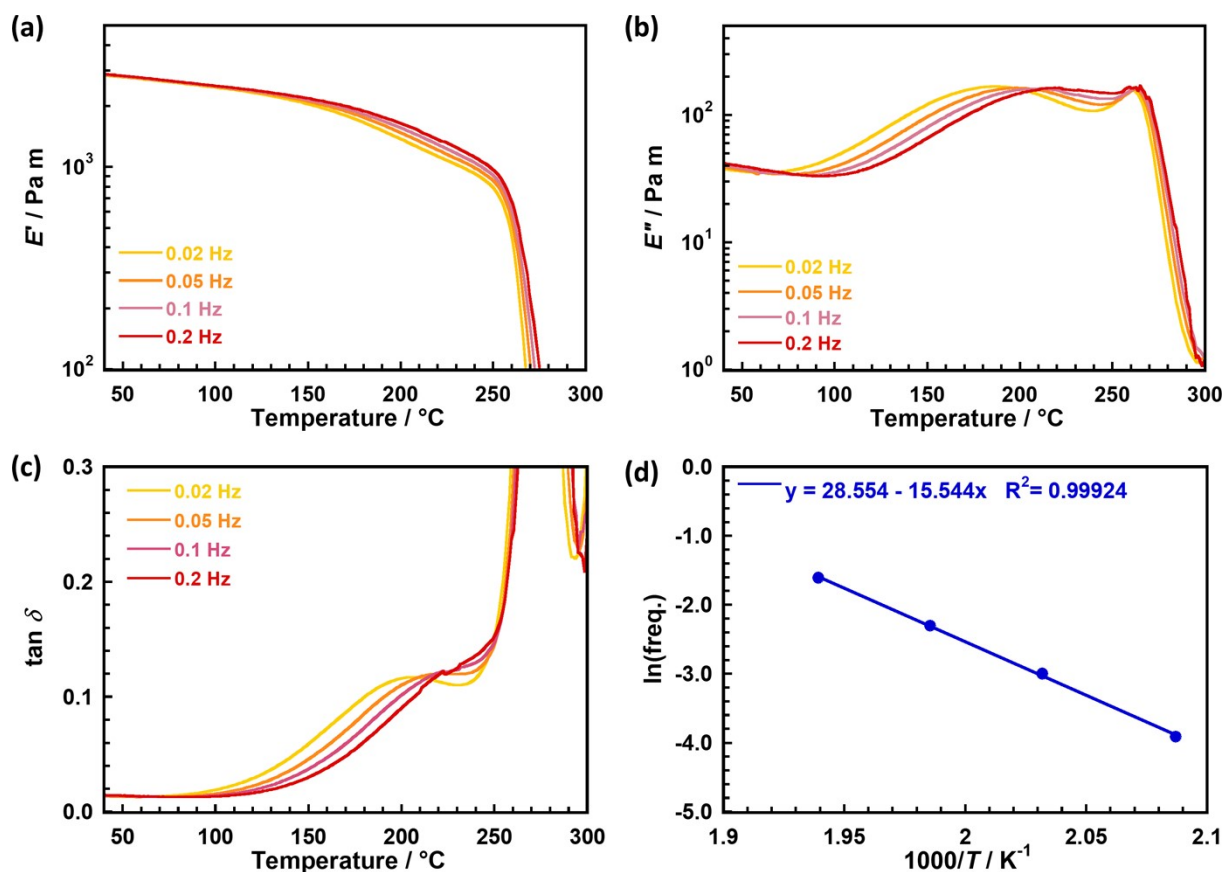
Figure S16. Temperature dependence of (a) storage modulus (E'), (b) loss modulus (E''), (c) tan δ, and (d) Arrhenius plot of ISS-TFDB measured at variable frequencies of 0.02–0.2 Hz.

Reference

(1)   Sawada, R.; Ando, S. Colorless, Low Dielectric, and Optically Active Semialicyclic Polyimides Incorporating a Biobased Isosorbide Moiety in the Main Chain. *Macromolecules* **2022**, *55* (15), 6787–6800. https://doi.org/10.1021/acs.macromol.2c01288.